arXiv:astro-ph/0011218v1 10 Nov 2000

Luminous compact galaxies at intermediate redshifts: progenitors of bulges of massive spirals ?

François Hammer[1] and Nicolas Gruel
DAEC, Observatoire de Paris-Meudon, 92195 Meudon, France

Trinh X. Thuan
Department of Astronomy, University of Virginia, Charlottesville, VA 22903

Hector Flores
Service d'Astrophysique, CEA-Saclay, 91191 Gif-sur-Yvette, France
and

Leopoldo Infante
Universidad Catolica, Santiago, Chile

ABSTRACT

VLT spectra of 14 luminous compact galaxies (LCGs) reveal strong metallic absorption line sytems as well as narrow and intense emission lines. Their gas extinction is found to be large ($A_V \sim 1.5$ mag) leading to an upward revision of their star formation rate (SFR) to an average value of $\sim 40\ M_\odot yr^{-1}$. Large extinction values are also supported by the large rate of detection in one field observed by ISO. Gas metal abundances in LCGs have about half the solar value. LCG absorption spectra can be synthesized with a mix of a few Gyr old and relatively metal-rich (generally solar to over-solar values) stellar population and a younger stellar population ($< 5\times10^8$ years) having a metal abundance similar to that of the gas.

We argue that LCGs are the progenitors of present-day spiral bulges. LCGs have masses and light concentrations similar to those of present-day bulges. They could have been formed entirely during a period of a few Gyr prior to the epoch of their observations if the star formation has been sustained at the observed rate. As in present-day galactic bulges, LCG stars show a wide range of abundances. Thus, observing LCGs allows us to directly witness an important stage in the formation of a massive galaxy, the building of the bulge prior to that of the disk. The gas needed to feed the observed star formation is likely to be falling in from the outskirts of the galaxy, being tidally pulled out from interacting companion galaxies. An infall scenario naturally explains the gas metal abundance which is generally lower than that of the older stellar component. At least for the strongest star-forming LCGs, there is clear imaging evidence for the presence of companions. Some LCGs also show evidence for the beginning of a disk formation.
If the above scenario holds for most LCGs, we estimate that at least 20% of present-day spiral galaxies have formed the bulk of their stars at relatively recent epochs, during the last 8-9 Gyr, at redshifts less than ~ 1. Since they are heavily extincted, we predict their IR luminosities to be relatively large, around $L_{IR}=10^{11}\ L_\odot$, i.e. near or slightly below the luminosities of the galaxies detected by ISO in the same redshift range. Taking into account the integrated IR luminosity of the LCG galaxy population can lead to a significant upward revision of the cosmic SFR density in the redshift range from 0.5 to 1.

Subject headings: galaxies: formation, galaxies: bulges

1. Introduction

The evolution of UV and IR luminosity densities can be understood as a decrease by a factor of $\sim$ 6 of the global star formation density from the epoch corresponding to redshift z=1 to the present epoch (Lilly et al. 1996; Flores et al. 1999). These luminosity densities evolve similarly and contribute equally to the star formation in that redshift range, if one assumes that the shapes of the UV and IR luminosity functions to be similar to the local ones (Hammer 1999). Integration of the derived global star formation implies that between half and two thirds of the present-day stars have been formed since z=1. This is somewhat in contradiction with the primordial collapse scenario in which the most massive galaxies were formed at much earlier epochs, at redshifts larger than $\sim$ 3 (e.g. Renzini and Cimatti 1999). The latter scenario is supported by the apparent non-evolution in the number density of large disks (Lilly et al. 1998), and by its success in reproducing galactic disk evolution with chemical evolution models normalized to local galaxies (Boissier and Prantzos 2000).

The study of the luminosity density evolution relies on observations of luminous galaxies with M_B < -20 in the optical, and with $L_{bol} > 2 \times 10^{11}$ $L_\odot$ in the IR. The two main galaxy populations responsible for the observed decline in the star formation density are, in decreasing importance, the luminous IR galaxies (Flores et al. 1999) and the luminous compact galaxies (LCG) (Guzman et al. 1997; Lilly et al. 1998). The former are generally large and massive galaxies found mostly in interacting systems (Hammer, 1999), and which show star formation rates (SFR) exceeding 50 $M_\odot yr^{-1}$. They represent $\sim$ 4% of the field galaxy population. The latter are much more numerous and contribute to more than 40% of the UV luminosity density at z$\sim$ 1 (Guzman et al. 1997; Hammer & Flores 1998). They constitute the most rapidly evolving galaxy population seen in the UV. The properties of these LCGs are still largely unknown. They are sometimes so compact that their nucleus is barely resolved in the WFPC2 HST images, which prevents their classification on the basis of their luminosity profile.

Koo & Kron (1981) first drew attention to these compact galaxies during their search for faint QSOs on the basis of colors and compactness. They identified a sparse population (the surface density is $\sim$ 30 sources per square degree) of very blue compact galaxies with z $\leq$ 0.7 and exhibiting narrow emission lines. Using the Keck HIRES spectrograph, Koo et al. (1995) demonstrated that the emission lines of LCGs have a Gaussian profile, and suggested that they may be progenitors of local spheroidal galaxies through fading by $\sim$ 4 to 5 magnitudes. More recently, Guzman et al. (1997) and Phillips et al. (1997) have identified a large population of emission-line compact galaxies in the flanking fields around the Hubble Deep Field (HDF, Williams et al. 1996) at z $\leq$ 1, comprising $\sim$ 20% of the field galaxy population. They found the [OII]λ3727 emission-line velocity widths of the compact galaxies to range between 35 and 150 km s^{-1} (Phillips et al. 1997), comparable to those of local dwarf galaxies, although the compact galaxies are 10 to 100 hundred times more luminous (up to a few $L^\star$). The similarities between the HDF compact galaxies and those from Koo and Kron (1981) have led Guzman (1999) to suggest that blue compact galaxies at intermediate redshifts may be the progenitors of local spheroidal or irregular galaxies through fading by $\leq$ 4 magnitudes. If true, according to Guzman (1999), these should have extremely low M/L ratio, and this scenario would imply a severe downwards revision of the amount of star formation at z$\sim$ 1, since the baryonic content in irregulars (or spheroidals) is very small (Fukugita et al. 1998).

We develop in this paper a different scenario for the nature of the brightest LCGs, which are major contributors to the observed decline of star formation density since z=1. In our picture, LCGs are not the progenitors of present-day spheroidal and irregular galaxies, but rather of today's spiral bulges which built up gradually over time by a series of mergers of smaller units. There have been several previous observations that have hinted at that scenario, but their meaning was not realized

[1]Visiting Astronomer, Very Large Telescope, operated by The European Southern Observatory

at the time. Thus, Phillips and al. (1997) found that a large fraction of galaxies selected by their compactness appeared to be small but bright spirals. Even adding a color criterion is not sufficient to distinguish between old and young stellar populations: Schade et al. (1999) found that fully a third of the distant ellipticals they studied show star formation and colors as blue as those of blue compact galaxies. The merging scenario comes naturally as the merging rate was about ten times higher at z=1 than it is today (Le Fèvre et al. 2000). Moreover, Guzman (1999) and Hammer (1999) have noticed that a large fraction of compact galaxies selected from the HDF and Canada-France redshift survey (CFRS) fields are in interacting systems, with the presence of complex and distorted features surrounding their cores. Finally, the LCGs in the CFRS fields have near-IR and visible colors very similar to those of other luminous non-dwarf galaxies, with values apparently not consistent with those produced by a strong and short burst of star formation in a low-mass object (Hammer et al. 1997). We present next new observational data which support and sharpen the above scenario.
In the following, h_{50}=$H_0/50$ and if not specified we adopt h_{50}=1 and q_0=0.5.

2. The sample: selection criteria

Our LCG sample was selected from two galaxy fields studied in the CFRS: the CFRS 0300+00 (Hammer et al. 1995) and the CFRS 2230+00 (Lilly et al. 1995) fields. To define our sample, we apply 3 selection criteria. First is the compactness criterion, as determined from deep HST images (see Brinchmann et al. 1998), or from deep ground-based images obtained by the CFRS team, with an image quality better than 0".8 FWHM and a pixel size of 0.207". It is based on either a small size:

$r_{1/2} \leq 5\ h_{50}^{-1}$ kpc, where $r_{1/2}$ is the half-light radius and h_{50} the Hubble constant in units of 50 km s^{-1} Mpc^{-1}

or on light concentration as defined by the parameter:

δ I = $m_I(15h_{50}^{-1}kpc)$ - $m_I(5h_{50}^{-1}kpc) \leq 0.75$ mag (Hammer and Flores 1998).

Imagery from HST has been analysed with SExtractor software package (Bertin and Arnouts, 1996). The detection threshold was set to3.5 σ and a 35 pixel annulus was used for sampling the background. The minimum contrast parameter for deblending was set to 0.005, and for each source with an identified companion at more than 2" (18 kpc at z=0.5), an image with a mask superimposed on the companion has been generated. The background level at the mask location has been set using the background mean level, and the mask size was set from the derived Kron radius of the companion (Bertin and Arnouts 1996). This procedure has the advantage of eliminating systematic biases against compact sources with companions beyond 2". For HST images, 15 apertures with diameters varying from 0".2 to 3".0 with increasing steps of 0".2, were used to derive aperture photometry. The half-light radius has been derived assuming that the isophotal magnitude generated by SExtractor was a good approximation to the total magnitude of the source. Calculation of the light concentration parameter was done after interpolating to the luminosities enclosed within the 5 kpc and 15 kpc radii. Ground-based images were analyzed in a similar way, but a 20-pixel annulus was used for background sampling. Another problem with images obtained from the ground come from background fluctuations. For the majority of the objects, aperture magnitudes are increasing smoothly with aperture radius. Those that show a magnitude decrease larger than the measurement errors have been excluded from the sample.

The above selection criteria are equivalent for a face-on disk or a spheroidal component with a $r^{1/4}$ profile since for a $r_{1/2} \leq 5$ kpc source, $m_I(15h_{50}^{-1}kpc)$ is a good approximation of the total source luminosity. Figure 1 demonstrates this equivalence for sources imaged with the HST. The bottom panel shows that the light concentrations calculated from HST and CFHT images for the same object correlate well, the correlation coefficient being 0.73. We note however that the average value of δ I from ground images is larger by 0.1 magnitude as compared to that from the HST images. This can be easily explained by the broadening of the profile due to seeing conditions, and we have applied a slight empirical correction to the

values derived from the ground. The correlation between ground and HST data is found to be better for the concentration parameter (upper panel) than for the half-light radius. We interpret this to be related to the uncertainties in the calculation of the isophotal magnitudes for ground-based images, because background fluctuations affect them more than aperture magnitudes. As a result, we have decided to adopt the concentration parameter as the selection criterion for compact galaxies. Examination of images of the selected compact galaxies shows that the compactness selection criterion has also picked out a few highly inclined disks with a large major axis extent. These were removed from the sample using the axis ratio calculated by SExtractor. One can also notice from Figure 1 that $\sim$ 20% of the sources are found to be compact on the basis of their HST photometry, although they appear to be extended from the ground. Examination of their images show that they are mostly sources with nearby companions (within 3") for which the deblending procedure applied to ground-based images has failed. In other words, our procedure applied to ground-based images appears to be more restrictive than when applied to higher spatial resolution HST images. A selection from ground images will inevitably generate a sample of galaxies slightly biased against galaxies with nearby companions.

Second, we apply a luminosity and redshift criterion. Only galaxies with M_{AB}(B) $\leq$ -20, and in the redshift range from 0.45 to 0.8 are included. The luminosity cut-off is motivated by the fact that the reported evolution of the rest-frame UV luminosity density is based on observations of galaxies with M_{AB}(B) $\leq$ -20 (Lilly et al. 1996), while the redshift range is the one in which the CFRS is considered complete for luminous galaxies (see Hammer et al. 1997).

Third, we include only LCGs with known [OII]λ3727 emission ($W_0([OII]) \geq 15$ Å), because we wish to compare the gas properties to those of the underlying stellar population.

Applying these three selection criteria to the 2 CFRS fields yields a sample of 59 galaxies, of which we have chosen a small representative subsample of 14 LCGs for a first investigation. They represent $\sim$ 23% of the M_{AB}(B) $\leq$ -20 galaxy population in the redshift range defined above. Their global properties, including B and K luminosities and compactness and concentration parameters, are given in Table 1.

Their apparent magnitudes range from I = 20.5 mag to 22 mag, and they possess colors spanning the entire morphological sequence from Irr to Sbc galaxies. They are very similar in their properties to the brightest $\sim$ 25% of the blue compact galaxies selected by Guzman et al. (1997) in the Hubble Deep Field at 0.1<z<1.3. However most of the brightest compact galaxies of Guzman et al. have higher redshifts than the LCGs considered here, which complicates a direct comparison.

3. Observations and data reduction

Spectrophotometric observations of the 14 LCGs were obtained during one night (1999 August 10-11) with the European Southern Observatory 8m VLT/UT1 using the FORS1/R600 and I600 spectrograph at a resolution of 5Å and covering the wavelength range from 5500 to 9200Å. This ensures the coverage from [OII]λ3727 to [OIII]λ5007 in the rest-frame spectrum for a large fraction of the targets. Additional exposures have been done through service observing mode, during July and August 2000. Each galaxy was observed through a 1" slit (Figure 2) in 5 to 7 exposures of $\sim$ 40 mn each, using the "shift and add" technique to ensure proper removal of cosmic rays and of possible CCD defaults. Spectra were extracted and wavelength-calibrated using the IRAF[1] package. Flux calibration was done using 15 min exposures of three different photometric standard stars. To ensure the reliability of the data, all spectrum extractions as well as lines measurements using the SPLOT program were performed independently by two of us (F.H. and N.G.).

To disentangle the continuum properties from those of the emission lines, we have adopted the following specific procedure for all spectra. We applied a two-step smoothing (first by 7 pixels and then by 15 pixels) to the continuum, while excluding from the smoothing the well identified

[1]IRAF is distributed by National Optical Astronomical Observatories, which is operated by the Association of Universities for Research in Astronomy, Inc., under cooperative agreement with the National Science Foundation.

and mostly unresolved emission lines to keep their original spectral resolution. This smoothing procedure has the advantage of not affecting the shape of the continuum and the narrow emission lines, while revealing the more prominent absorption features. For the latter the nominal spectral resolution is $\sim$ 10 – 11 Å, comparable to that of the stellar cluster spectra used as templates in our spectral synthesis work to be described later (section 4.2). Figure 3 presents the 14 resulting rest-frame spectra, where the location of strong sky emission lines (at 5577, 6300 and 6364Å) as well as sky absorption lines (at 6874, 7590 and 7630Å) have been indicated. Excluding these night sky lines, the smoothed continuum of all spectra shows a S/N per pixel element always larger than 5. For each spectrum, the locations of the most prominent lines are marked and their identifications are given in the last panel.

The $H\beta$, $H\gamma$ and $H\delta$ Balmer emission lines were found to be systematically contaminated by absorption lines. To disentangle the absorption from the emission, we have synthesized the stellar continuum by a combination of star spectra. Stellar energy distributions were taken from the library of Jacoby et al. (1984). The stars have solar metallicity which is appropriate for our objects as shown later. We used a combination of stars with spectral type varying from B to K, and optimized the fit to the continuum for the important spectral absorption lines, such as the high order Balmer lines (H10 to H8), the CaII K line and the G band (Figure 4, top panel). We impose the additional constraint that the resulting synthesized stellar continuum not be redder than the object continuum, since the spectra of LCGs have simultaneously strong absorption features characteristic of old stellar populations and blue U-V colors characteristic of young ones. The synthesized stellar continuum is then subtracted from the observed spectrum to yield a pure emission spectrum uncontaminated by absorption (Figure 4, bottom panel) which we can use to measure the Balmer decrement and derive extinction. For 12 LCG spectra with both Hβ and Hγ lines, the residual emission lines have been measured using the SPLOT package, and the measurement errors estimated by trying several combinations of the stellar templates. In most cases, the Balmer emission lines are seen to be either blue or red-shifted with respect to the center of the absorption lines, which minimize their contamination by underlying stellar absorption, and hence the measurement error for the gas extinction.

Emission line widths were estimated after a careful examination of the actual spectral resolution because seeing conditions were varying from 0".65 to 1".0 FWHM, and the object sizes were comparable to the slit size. The instrumental resolution is around 5 Å (FWHM), as measured from absorption lines of the calibration stars and unresolved sky lines. Each line measurement was checked against the closest sky emission line and velocity widths were derived assuming a gaussian profile. All spectra but one include the [OIII]λ4959 and 5007 emission lines. Following Guzman et al. (1997), velocity widths derived from this set of lines are averages, weighted by the quality of individual measurements. They are given in Table 2.

4. Stellar populations

4.1. Color properties

Ten of the 14 LCGs possess K' band photometry (Hammer et al. 1997) along with B, V and I photometry. At the reference redshift of z = 0.5182, the central wavelength of the observed I band is exactly that of the rest frame V band, while the observed V band matches well the rest frame U band centered at 3622 Å. At this redshift the observed K' band represents a filter centered around 1.416 μm. Observed colors have been derived within an aperture of 3" diameter. Calculations of rest-frame colors has been done by systematic fits of the observed V, I and K' photometric points, using Bruzual and Charlot (2000) models with exponentially decreasing SFR characterized by e-folding times τ of 0, 0.1 Gyr, 0.5 Gyr, 1.2 Gyr, 4 Gyr and infinity. The fits have been performed without extinction correction, and reproduce well the colors of all objects except for CFRS 03.1349, CFRS 03.1540 and CFRS 22.1064. The latter objects have observed (I - K') colors which are too red even when compared with those of a 15 Gyr old stellar population. Because the 14 selected LCGs have redshifts close to the reference one, the model-dependent corrections applied to

the rest-frame colors (U - V) and (V - 1.4 μm) are always negligible or smaller than the measurements errors (i.e. < 0.05 mag). Thus, our derived rest-frame colors are very accurate, with only a second-order dependency on the model used to derive them.

The resulting color distribution in Figure 5 illustrates the following point: our sample which was constructed using a selection criterion on the emission lines includes galaxies with (U - V) colors ranging from those of Irr to those of Sbc, just as the sample of Guzman et al. (1997). On the other hand, our LCGs display a large dispersion of the (V - 1.4 μm) color, with 7 of them showing colors much too red compared to the predictions of the models. Model uncertainties of the (V - K) color – which is very similar to the (V - 1.4μm) color – cannot account for this effect. These very red colors can be explained if the presently observed burst is superimposed on a red old stellar population, if there is significant extinction, if the stellar population has over-solar abundances, or if there is a combination of the above. For the reddest objects (CFRS 03.1242, CFRS 03.1349, CFRS 03.1540 and CFRS 22.1064), a combination of these effects is likely at work. Interestingly, these four extremely red LCGs all possess a bright companion within 4" or 36 kpc (Figure 2). These companions are not affecting the K' band aperture photometry, except maybe for 03.1242. The CFRS 0300+00 field was also observed by ISO to a limit of 350 μJy (4σ) at 15μm and by the VLA to a limit of 90μJy (5σ) at 21 cm. Two very red LCGs, CFRS03.1349, 03.1540 in our sample have been detected at both mid-IR and radio wavelengths.

The dispersion in the (V - 1.4 μm) color justifies *a posteriori* our adopted name for these objects, Luminous Compact Galaxies (and not blue LCGs), since only their (U-V) colors are blue. The lower luminosity compact galaxies of Guzman et al. are significantly bluer in (V - 1.4μm) as compared to the LCGs in our sample (Guzman, private communication).

4.2. Absorption lines

All the LCG spectra show strong and broad absorption lines. Most prominent are the Balmer lines, the Ca I 4227Å and Ca II H and K lines, the CN band at 4182Å, the CH band at 4301Å, and the Mg I line at 5173Å (Figure 3). A special mention should also be made for the important iron absorption line system in LCG spectra, including Fe I 4037Å , 4264Å , 4384Å and 4435Å, and sometimes Fe I 4004Å , 4595Å and 4645Å . FeI lines are even present below 3900 Å . This suggests that a large fraction of stars in LCGs have solar abundances or greater, and that SN Ia have already released iron-peak elements, giving an age of about 1 Gyr or more for the bulk of the stars (see e.g. McWilliams 1997). In some LCG spectra the CN band affects the location and shape of the H8 and H9 lines (see for example the spectrum of 03.1540), which also suggests the presence of high metal abundance stars.

Table 3 gives the equivalent widths of the most important absorption lines. The continuum has been synthesized using a grid of stellar cluster spectra with different ages and metallicities, and following the procedure outlined by Bica & Alloin (1986a and b, herafter BAa and BAb). To test our computer routines, we have first performed a continuum fit of the stellar cluster spectra, and check our results against those of BAa, before applying the procedure on LCG spectra. Our measurement errors are slightly lower than those of BAb 's Table 5 (from 1 to 2 Å). We found a correlation between the equivalent widths of the metal absorption lines and the $(V - 1.4\mu\mathrm{m})_{AB}$ color index (Figure 6). This is to be expected if the latter is mainly sensitive to age and metallicity effects. A few objects depart from the correlation. These are the reddest LCGs, CFRS03.1349 and 22.1064, for which we suspect extinction to modify the $(V - 1.4\mu\mathrm{m})_{AB}$ color index. Figure 6 also shows that the properties of most LCGs are consistent with their stellar populations being composed of a 5 Gyr old population with solar abundance, mixed with a young ($\leq$0.1 Gyr) population, the latter being responsible for the dilution of the absorption lines.

The Bica & Alloin population synthesis method allows us to perform a two-parameter analysis which takes into account both age and metallicity effects. Because galaxy interactions are important

in LCGs, we prefer not to adopt any assumption concerning the abundances of the young population relative to those of the old population, as done by Bica (1988) in his analysis of E/S0 and spiral nuclei. On the other hand, to simplify the analysis, we have made the plausible assumption that, in a small volume with intense star formation, the gas is chemically homogeneous at least during the last 10^8 years. Ten absorption lines have been used to perform the fit. They include H 10 (3798 Å), H8 (3889 Å), Ca II K (3933 Å), FeI (4037 Å), CN (4182 Å), CaI (4227 Å), FeI (4264 Å), the G band (4301 Å), FeI (4384 Å) and MgI (5175 Å). For most LCGs, this results in 4 to 7 lines available in the spectral range, and not contaminated by sky emission or absorption. Five star cluster populations with ages 5×10^9, 10^9, 5×10^8, 10^7 and 10^6 yr have been used as templates. We have chosen not to use globular cluster spectra (age = 15×10^9) because at z$\sim$ 0.5, LCGs emitted their light not more than 6-7 Gyr ago. The metal abundance of the older population was allowed to be one of the following values: $log(Z/Z_\odot)$ = - 1.5, - 1, - 0.5, 0 and 0.6. The same metal abundance has been assumed for the 10^9 and 5×10^8 yr old populations ($log(Z/Z_\odot)$= -1, -0.5, 0 and 0.6), and for the 10^8 and 10^7 yr old populations ($log(Z/Z_\odot)$ = -0.5, 0 and 0.6). Our goal here is not to fully disentangle the metallicity from age effects for each LCG (our spectra do not have the required S/N to accomplish that), but rather to have a first rough estimate of its stellar population properties. In many cases, LCGs show large equivalent widths of FeI 4384Å and MgI 5175Å and relatively small equivalent widths of CaII K lines. The latter have been fitted thanks to the line dilution in the blue by the younger population which has a HII spectrum. The fit has been done as follows: we add first a new star cluster population to the mixture in incremental steps of 5% in the light contribution. If the objects are not fitted, we reduced the step to 2%. In some cases, the individual iron line equivalent widths were not well reproduced by the models. This is not too surprising given the complexity of the Fe line system: even for well-known stars, Fe/H is not known to better than a factor of 2 or 3 (Wheeler, Sneden & Truran 1989). For the 6 LCGs with non-satisfactory fits of individual Fe lines, we have fitted only the sum of the three FeI rather than each of them individually.

Table 4 presents the result of the fits. χ^2 values are calculated as averages of the sum of the squares of the differences between model and LCG spectrum divided by the squares of the measurement errors. The latter are taken to be the quadratic sum of the BAb errors and our errors. We also restrict the parameter space to be explored by imposing the plausible constraint that the (3728Å - 5175Å) color (approximately the (U-V) color) of the model has to be bluer than that of the LCG. The contribution to the V light of each population in the synthesis model is given in Table 4, in bold characters for the major contributor. Most LCGs are dominated by populations having ages ranging from 1 to 5 Gyr. We have tested this result by attempting to fit the LCG absorption lines by limiting the age range to values lower than or equal to 5×10^8 yr : for all LCGs but CFRS 22.0637 and CFRS 22.0919, the χ^2 value of the fit is well in excess of 1.

Except for CFRS 22.0637 and CFRS 22.0919, the stellar populations in LCGs invariably include an important contribution ($\geq$ 35%) stars older than 1 Gyr and with metal abundance $log(Z/Z_\odot)$ $\geq$ -0.5. For 9 of them, we find an important contribution of $>$ 1Gyr stars with $log(Z/Z_\odot) \geq 0$. We have tested the robustness of the latter result by running models where the metal abundance has been constrained to have $log(Z/Z_\odot)$ values lower than or equal than -0.5. We found that for 7 LCGs, CFRS 03.0523, CFRS 03.0570, CFRS 03.0595, CFRS 03.1242, CFRS 22.0344, CFRS 22.0429 and CFRS 22.0619, there is no possibility to fit their absorption line spectra without an important contribution of solar or oversolar stellar population. Special mention should be made of CFRS 03.1242 for which we could not find a satisfactory fit. The reason is that it shows very strong absorption lines (Table 3), stronger than the most metal-rich star clusters in our library. Four LCGs, CFRS 03.1540, CFRS 22.0637, CFRS 22.0919 and CFRS 22.1064, apparently require low-abundance populations to fit their absorption line spectra. However our modelling was unsuccessful to provide physical solutions for CFRS 03.1540 and CFRS 22.1064, for which no (or in very small amounts) young population responsible of their emission lines have been identified. Any young component added would dilute the absorption lines, and would lead to an old

stellar component with a solar metallicity.

While our spectral synthesis work allows us to put constraints on the ages and metallicities of the stellar populations in LCGs, the reader should not take the values given in Table 4 as being the actual stellar population distributions in LCGs. There are several caveats which limit the results of our adopted spectral synthesis procedure. First, there is more than one solution with χ^2 values lower than 1, and Table 4 only displays the solution with the minimum value. These appear to be true minima as they do not change when the incremental step for adding the light contribution of a stellar population is changed. Second, the fit of a galaxy population using only a few stellar cluster templates can smooth over some important events in the star formation history of a galaxy in which star formation is sustained over long periods of time. We believe this effect to be especially important in LCGs within interacting systems. The complex nature of the star formation history and the resulting young stellar population could then explain its absence in CFRS03.1540 and CFRS 22.1064. It can also be the reason why our modeling of CFRS 03.1242 proves to be unsuccessful. Third, and more importantly, our ability in disentangling age from metal abundance effects is limited by the relatively small number of absorption lines. For example, some LCG spectra do not cover the blue region and do not include the important lines below 4000Å. This would bias the synthesis method against finding young stellar populations which would dilute the UV absorption lines. This effect can be seen in Table 4 for CFRS 03.1540 and CFRS 22.1064 for which the best-fit model found no young population, although their spectra show emission lines. What can be firmly said about the metal abundance and age of LCGs ? First, all LCGs, but CFRS 22.0637 and CFRS 22.0919, are dominated by 1 to 5 Gyr old population, characterized in most cases by solar to over-solar abundances. To test the robustness of this result, we have attempted to fit the 12 LCGs with an old stellar population with the added constraint that the contribution of that old population does not exceed 25%. We found that half of the LCGs spectra could not be fitted, their χ^2 being invariably greater than 1. As for the remaining LCGs, they could be only fitted by assuming a young population with the highest metal abundance available in our stellar library ($log(Z/Z_{\odot}) = 0.6$). This is not realistic when compared to the gas abundance values discussed in the next section. Second, the best fits to the LCGs spectra always give a mix of stellar populations with metal abundance covering a wide range from undersolar (generally characterizing the youngest population) to solar or oversolar values (characterizing the oldest population). This is illustrated in Figure 6, which shows that the most important lines within a LCG cannot all be fitted with a single metallicity. As noted above, some models of LCG spectra show no young population, in evident contrast with their emission line spectra. Adding a young stellar component would inevitably enhance the metal abundance of the oldest stellar component, making our conclusion that most LCGs are dominated by old and solar metallicity stellar population even stronger.

5. Gas properties: SFR and oxygen abundance

For the 12 spectra with both $H\beta$ and $H\gamma$ detected, we have been able to derive A_V extinction values, after correcting the Balmer emission lines for stellar absorption using the results of our spectral synthesis work (Section 3). As shown in Table 5 and Figure 7 (left panel), the derived extinctions can have values much larger than those currently found in present-day irregular galaxies which have an average A_V of ~ 0.57 (Gallagher et al. 1989). These large extinctions imply that the SFR derived from the 2800Å luminosity of LCGs is greatly underestimated. We have calculated for each LCG the dereddened $H\beta$ line flux and derived the corresponding SFR using a Salpeter IMF (Kennicutt 1998) and assuming the standard ratio between $H\alpha$ and $H\beta$, Case B and a gas temperature of 10000 K. Figure 7 (right panel) compares the SFRs so calculated to those derived using the 2800Å continuum, assuming the same IMF (see Kennicutt 1998). Even allowing for errors due mainly to uncertainties in the extinction estimates, it is clear that the UV luminosity underestimates the actual SFR in LCGs by factors ranging from 2 to 30, with an average of 14 and a median of 11. The largest underestimates are for CFRS 03.0523, CFRS 03.1540 and CFRS 03.1349, which are both IR-luminous galaxies. From their IR and radio energy distributions, Flores & Hammer (2000, in preparation) derive SFRs respec-

tively of 87, 135 and 94 $M_{\odot}yr^{-1}$. These values are in agreement with those derived from the extinction corrected Balmer lines, allowing for the error bars which have large upper values. As another consistency check, we have applied the extinction factor derived from the $H\beta/H\gamma$ ratio to correct the SFR values at 2800Å (see Table 5). Extinction-corrected SFR_{2800} values are always consistent with extinction-corrected $SFR_{H\alpha}$ values within the error bars.

The O/H abundance ratio for the gas can be estimated from the quantity $R_{23} = ([OII]3727 + [OIII]4959,5007)/H\beta$ (Edmunds and Pagel 1984), although the relationship is degenerate and there are two O/H values for a given R_{23}. The calculated R_{23} for the 12 LCGs with the necessary lines range from 0.5 to 1 (Table 6), in good agreement with the values obtained for similar objects at lower redshifts by Kobulnicky and Zaritsky (1999). Flux measurements of the faint [OIII]λ4363 line allow to lift the degeneracy for two objects (CFRS22.0619 and CFRS22.0919). For those, we derive gas temperatures of 12500 and 13000 K, close to the average upper value for the rest of the sample (Table 6). Using Figure 8 of Kobulnicky et al (1999), it was possible to set for each line ratio R_{23}, an upper and a lower value of O/H, with the help of the ionisation ratio $[OIII]4959,5007/[OII]3727$. We found that all LCGs have gas abundances $Z/Z_{\odot}$ in the range from 0.25 to 0.4, with the exception of CFRS 22.0919, to be discussed later, which shows a very low O/H. Adopting a statistical correction of +0.1 dex on the O/H abundance as suggested by Kobulnicky et al. (1999) for physical parameters derived from global galaxy spectra, our data are finally consistent with a median metal abundance $Z/Z_{\odot}$ = 0.45, similar to the value derived by Kobulnicky and Zaritsky (1999) for their objects. Thus, gas in LCGs displays oxygen abundances intermediate between those of local spirals ($Z/Z_{\odot} \sim 1$) and those of irregular dwarf galaxies ($Z/Z_{\odot} \sim 0.3$).

6. Discussion

We have obtained VLT spectra of 14 LCGs selected by their compactness and luminosity in the rest-frame blue. The blue luminosities of LCGs range from 0.35 to 1.4 $L^{\star}$ with an average of 0.70 $L^{\star}$. They are also bright in the near-IR, with a rest-frame K-band luminosity ranging from 0.1 to 2.8 $L^{\star}$ and an average of 0.86 $L^{\star}$, assuming $M_K^{\star}$(AB)=-22.55 for H_0 = 50 (Glazebrook et al, 1995). Guzman (1999) has noticed that LCGs are also compact at near-IR wavelengths. Here we assume that the K-light samples the stellar mass (Charlot 1998), with a mass-to-IR light ratio very close to unity. This follows Charlot (1996) who has investigated this ratio for a solar abundance population with various ages, appropriate for LCGs. A Salpeter Initial Mass Function (IMF) has been adopted, as it allows models to reproduce well the evolution of the global IR and B luminosity densities from z = 0 to z =1, to which the LCGs contribute importantly. On the other hand, Lilly et al. (1996) found that the use of a Scalo IMF in modeling the z = 0 – 1 galaxy population produces too many long-lived low-mass stars. Also photometric properties of local disks suggest a Salpeter rather than a Scalo IMF (Kennicutt et al. 1994). In any case, the adopted 0.22 dex uncertainty based on Charlot (1996)'s study of the conversion of K luminosity to mass likely accounts for the major uncertainties related to the IMF.

LCGs have stellar masses ranging from 10^{10} to 2.5 $\times 10^{11}$ $M_{\odot}$, with an average of 7 $\times 10^{10}$ $M_{\odot}$ (see Table 1). K-band luminosities derived from the 1.4μm luminosities are robust as the (1.4μm-K) color shows small variations during the period from 10^8 years (it has the value -0.32 mag) to 10^{10} years (its value is -0.15 mag) after the beginning of star formation. Uncertainties in these derivations are small compared to the large uncertainty involved in the conversion of the K-light into mass ($\sim$ 0.22 dex in Figure 8). From the way they have been selected and their properties, the LCGs studied here are very similar to the 25% most luminous blue compact galaxies identified by Guzman et al (1997) in the Hubble Deep Field (HDF). They are the galaxies responsible for the decrease in the UV luminosity density since the epoch corresponding to z=1 (Lilly et al. 1998).

With the noticeable exception of CFRS 22.0919 and CFRS 22.0637, LCGs all display strong metallic absorption lines and have (U-V) colors similar to those of late-type galaxies, in the range Sbc to Irr. These properties can be reproduced by a combination of an old star population with age $\geq 10^9$ yr with a younger population with age $\leq 5 \times 10^8$ yr (see Section 4.2). It is important to

note that the best spectral synthesis fits are generally obtained with an older stellar population with abundances larger than or equal to solar values, while the younger component has solar or sub-solar abundances. The latter component diminishes the observed strength of the absorption lines due to the older stellar population, as well as making the $(U-V)_{AB}$ color bluer than that of a Sbc galaxy. Analysis of the emission lines indicates that the ionized gas in LCGs also displays oxygen abundances in the range from 0.3 to 0.5 the solar value, i.e. the metal abundance of the gas is similar to that of the younger stellar population.

Given these observations, what can we say about the nature of LCGs? The presence of a moderately old stellar population with solar abundances or larger, stellar masses near that of the Milky Way, large SFRs similar to or only slightly below those of luminous IR galaxies, all argue against a scenario in which LCGs are progenitors of today's spheroidal or irregular dwarf galaxies as discussed by Koo et al. (1995) and Guzman et al. (1997). That hypothesis is based mainly on one key observation: that of the small velocity widths of the emission lines of LCGs (Table 2). These authors argue that the velocity widths are representative of virialized motions of the gas and since the velocity widths are similar to those of dwarf galaxies, they are dwarf progenitors. However an examination of the LCG spectra (Figure 3), shows that the Balmer emission lines are often red-shifted relatively to the Balmer absorption, suggesting that more complex mechanisms may be responsible of the narrowness of their widths. We also note that, in some cases, emission lines have asymetric profiles. In the case of CFRS 03.0523, they show two peaks separated by ~ 470 km s^{-1}, which are likely to be associated with each of the two merging components (Gruel et al. 2001, in preparation). A special comment should be made about CFRS 22.0637 and CFRS 22.0919 which, as we have noted before, appear to be different from other LCGs and resemble more HII galaxies. In particular, CFRS 22.0919 has a young low-metallicity stellar population as well as a low gas oxygen abundance, it shows a moderate gas extinction, and a large velocity difference (800 km s^{-1}) between the emission and absorption lines. Gas outflow can be responsible for the blue-shifted Balmer absorption lines, so that CFRS 22.0919 may be just the type of dwarf progenitor object discussed by Koo et al. (1995) and Guzman et al. (1997).

But objects such as CFRS 22.0919 constitute more the exception than the rule in our LCG sample. The stellar mass as well as the light concentration of other LCGs is more reminiscent of those of bulges of today's Sab to Sbc spirals or even ellipticals. Could LCGs be the progenitors of bulges of present-day massive galaxies? The bulk of their stars displays a large range in metal abundance, as in the Milky Way's bulge. Taking into account their large extinctions, LCGs are found to be still forming stars at a very vigorous rate, with a median SFR equal to 40 $M_{\odot} yr^{-1}$. For 8 LCGs with the necessary data, the median characteristic formation time scale for the bulk of the stars derived from the emission lines is ~ 1.8 Gyr (Figure 8). This value is consistent with that obtained by the absorption line analysis, but is much larger than the characteristic time of ~ 0.1 Gyr for the monolithic scenario of bulge formation (Elmegreen 1999). Thus, the latter scenario does not appear to be the appropriate one for explaining the observed properties of the majority of LCGs.

Which mechanism can then explain the transformation of LCGs to present-day spirals? An important hint can be obtained from HST images. These show that an important fraction, if not all, of the LCGs possess a low-surface-brightness component which surrounds their core (Figure 2, see also Guzman, 1999 or Hammer, 1999). Moreover, a substantial fraction of them (6/14) are seen to have bright companions within a radius of 40 kpc. The LCGs with companions show the largest SFRs in the sample, and they are also the reddest in (V-1.4μm). The three galaxies in the sample which have been detected by ISO (Flores et al. 2000, in preparation) are among them. It is thus plausible to think that gas tidally pulled out from the companion and falling into a LCG can feed the star formation within it. This would naturally explain the metal abundance difference between the gas and the oldest stars. A good example of a LCG where such a mechanism may be at work is CFRS 03.1540: its low-surface-brightness companion acts as a reservoir of low abundance gas to sustain the star formation in it during several 10^8 yr. CFRS 03.1540 also shows a well-developped disk – it was classified as a disk galaxy by Lilly et al.

(1998) – and star formation is probably occurring in both bulge and disk. The tadpole galaxies described by Brinchmann et al. (1998) which would have been selected as LCGs by our criteria, can be interpreted in this context as undergoing the first stage of the formation of a disk around the bulge. Thus, by observing LCGs, we are witnessing an important phase of galaxy formation: the building of the bulge and the beginning of the disk formation of $L^\star$ spirals, where galaxy interactions play a major role.

The scenario developped here has to account for the narrow emission line widths reported by Phillips et al. (1997) and also seen in several of our spectra. In normal galaxies, the bulge is dynamically relaxed, and the gas emission likely samples most of the velocity field, i.e. the emission line widths should be indicative of the whole galaxy potential. Weedman (1983) reported however unusually narrow emission line widths in starburst nuclei. Lehnert and Heckman (1996) studying a sample of IR-selected starburst galaxies, have shown that the starburst occurs preferentially in the inner region, so that the gas does not sample fully the solid body part of the rotation curve. They found several objects with emission line velocity widths of less than 50 km s^{-1} in systems with rotational velocities ranging from 100 to 200 km s^{-1}. Since they have SFRs and hence IR luminosities, equal or slightly below those of ISO galaxies (Flores et al. 1999), we conclude that our LCGs are very similar to some Lehnert & Heckman galaxies, and that the narrow emission line widths are not indicative of the entire potential of the LCGs and lead to a systematic underestimate of their true masses.

The present study thus suggests that LCGs are progenitors of today's massive (non-dwarf) galaxies, which have formed the bulk of their stars at z < 1. We note that:
1) the gas supplied to LCGs from interacting companions is enough to sustain their star formation during several 10^8 yr, until completion of the bulge stellar content as well as to feed a gradual formation of the disk.
2) the characteristic time for the formation of the bulk of LCG stars is relatively small, averaging to only $\sim$ 1.8 Gyr, i.e. most of the stars formed at z < 1.
Because LCGs represent $\sim$ 20% of the field galaxies, the fraction of stars in massive galaxies formed at relatively recent epochs could have reached 20%, and even more if the star formation in interacting systems of large (non-compact) galaxies detected by ISO (Flores et al. 1999; Hammer, 1999) is taken into account. This estimate is much higher than the one obtained by Brinchmann & Ellis (2000), who find the fraction to be negligible. The main reason for the discrepancy comes from the way the SFR is derived. Brinchmann and Ellis (2000) calculate the SFR from the [OII]3727 flux, while we use the extinction-corrected $H\alpha$ emission, assuming the standard ratio between $H\alpha$ and $H\beta$, Case B and T = 10000 K. Our derived SFRs can be a factor 10 or more greater than those derived by Brinchmann & Ellis (2000). This can be seen by comparing their Figure 3 to our Figure 8. Using the same sample as that of Brinchmann & Ellis (2000), Hammer and Flores (1998) have shown that SFRs derived from either [OII]3727 or 2800Å luminosities do not correlate with those obtained from $H\alpha$ luminosities, mainly because of extinction effects.

Given their large extinction and $H\alpha$-derived SFRs, it is likely that the IR luminosities of LCGs are similar to or only slightly below those of the luminous IR galaxies detected by ISO in the same redshift range (Flores et al. 1999). Because they represent 20% of the field galaxies in the redshift range from 0.4 to 0.8, the contribution of the LCGs to the global SFR density needs to be reevaluated. Such a reevaluation will probably lead to an increase in the fraction of the SFR density related to photons reprocessed by dust, i.e. there should be an evolution in the shape of the IR luminosity function, due to the addition of new populations – such as LCGs – around L_{IR}=$10^{11} L_\odot$. This subject cannot be addressed properly with our present small sample. We shall discuss it in a future paper with a much enlarged sample.

7. Conclusions

Spectroscopic observations of a small sample of 14 Luminous Compact Galaxies (LCG) with the VLT have provided new and important information on a crucial stage in the formation of galaxies, that of bulges in massive (non-dwarf) spiral galaxies. The LCG spectra are characterized by the following properties:

1) they show strong metallic absorption lines, including those from α-elements and iron.

2) they show large Balmer decrement ratios (as measured by $H\beta/H\gamma$), implying large extinctions (median A_V of $\sim$ 1.5 mag).

3) the SFRs derived from the extinction-corrected Balmer lines are more than ten times higher than the corresponding ones derived from the UV luminosities.

LCGs with redshifts between 0.4 and 0.8 are undergoing intense bursts of star formation, with SFRs averaging to $\sim 40\ M_{\odot} yr^{-1}$. Because of their large extinctions, they are expected to be luminous in the IR, at a luminosity level just below the IR luminous galaxies detected by ISO in the same redshift range (Flores et al. 1999). Indeed 3 of the 14 LCGs discussed in this paper are detected by ISO, implying higher extinction for them.

We believe that LCGs are progenitors of present-day bulges of massive spiral galaxies because:

1) they have stellar masses similar to those of today's bulges in $\geq L^{\star}$ spirals, concentrated in comparable volumes.

2) their stars show a wide range of metal abundance, from sub-solar to over-solar values, as in the bulge of the Milky Way.

3) the majority of LCGs show low-surface-brightness components around their high-surface-brightness cores (the bulges). Most are in interacting systems, and the tidally pulled gas from the companions is likely to sustain star formation in the LCGs at a high rate for several hundreds Myr, resulting in the completion of the bulge formation and the beginning of the disk formation. The characteristic time for forming the bulk of the stars in LCGs is rather small, only $\sim$ 1.6 Gyr on average. It is comparable to the age of the oldest stars in LCGs derived from the analysis of their absorption lines. This means that a significant fraction (several tens of percent) of present day's massive galaxies could have been formed at relatively recent epochs, at z $\leq$ 1. This is consistent with the cosmic star formation history which predicts that an important fraction of the stellar mass was formed in the z = 0 – 1 redshift range (Hammer 1999). The importance role played by galaxy interactions in the formation of bulges of spiral galaxies is also consistent with the hierarchical theory of galaxy formation. On the other hand, the scenario outlined here may appear to be in contradiction with the results of Lilly et al. (1998) who found that the number density of large spirals at z $\sim$ 1 is comparable to that today. However the Lilly et al. results are based on only $\sim$ 40 morphologically selected large spirals in the redshift range from 0.2 to 1, and their large one σ error bar can easily accomodate a density evolution of spiral disks of $\sim$ 20% as found here. Moreover, some of the large spirals in Lilly et al. (1998)' sample are in interacting systems and are strong infrared emittors, such as CFRS 03.1540 discussed here, or other examples discussed by Flores et al. (1999). Presumably, these large interacting disks will merge leading to a density evolution.

If the 14 LCGs described here are representative of the whole LCG population at z >0.4, then their contribution to the global star formation density should be revised upwards by factors as large as 7 – 10. That contribution could then be as high or higher than that of the luminous IR galaxies detected by ISO (Flores et al. 1999). The latter are more massive systems and formed stars more rapidly than LCGs, but they constitute a much sparser population of galaxies, comprising only a few percent of the total population. Most LCGs at z $\sim$ 0.5 would have bolometric IR luminosities not far below the ISO sensitivity limit, and we predict that they will be easily detected in large numbers by SIRTF.

Finally we reiterate that our interpretation of the nature of LCGs is quite different from that proposed by Koo et al. (1995), Guzman et al. (1997) and Guzman (1999) for the majority of compact galaxies found in the Hubble Deep Field and flanking fields. This is probably because most of the Guzman et al galaxies have intrinsically lower luminosities than LCGs. We believe LCGs to be 10 to 100 times more massive than dwarf galaxies, to be forming stars at large rates, so they cannot be the progenitors of local spheroidal or irregular systems through fading. Corresponding to the brightest 25% of the compact galaxies selected by Guzman et al (1997), the LCGs selected in CFRS fields are mostly evolved starbursts probably similar to those classified as such in the HDF. Due to their large derived SFRs, LCGs are the main contributors to the large SFR density observed at z=0.5 to 1.

In future papers (Gruel et al. in preparation) we will investigate the velocity fields and dynamics of LCGs, using data of superior quality and based on a larger sample. We will also be studying the possible revision of the star formation history and of the IR luminosity density caused by the LCG population.

We are grateful to C. Balkowski, F. Combes, R. Guzman, D. Kunth and C. Vanderriest for useful discussions and advices. We are especially indebted to Pascale Jablonka who introduced us to the methodology of fitting absorption line spectra by star cluster synthesis. We thank the ESO Allocation Time Committee for the one night attributed to this program at UT1. F.H. is very grateful to Claire Moutou and Thomas Szeifert for their help at Paranal and their patience. We thank the data flow operations team for the fast delivery of the data. We thank the CNRS/CONICYT for financial support of our collaboration. T.X.T. is grateful for the hospitality of the Departement d'Astronomie Extragalactique et de Cosmologie at the Observatoire de Meudon and the Institut d'Astrophysique during his sabbatical leave. He thanks the partial financial support of the Centre National de la Recherche Scientifique, of the Université of Paris VII and of a Sesquicentennial Fellowship from the University of Virginia.

REFERENCES

Bertin, E., & Arnouts, S. 1996, A&A, 117, 393

Bica, E., & Alloin, D. 1986a, A&A, 162, 21

Bica, E., & Alloin, D. 1986b, A&AS, 66, 171

Bica, E. 1988, A&A, 195, 76

Boissier, S., & Prantzos, N. 2000, MNRAS, submitted

Brinchmann, J., et al. 1998, ApJ, 499 112

Brinchmann, J., & Ellis, R. 2000, ApJ, 536, 77

Bruzual, G., & Charlot, S. 2000, in preparation

Charlot, S., 1996, in the Universe at High-z: Large Scale Structures and Cosmic Microwave Background, ed. Martinez Gonzales & J. Sanz (Berlin : Springer), 53

Charlot, S., 1998, in The Next Generation Space Telescope: Science Drivers and Technological Challenges, 34th Liege Astrophysics Colloquium, 135 (astro-ph/9810408)

Charlot, S., Worthey, G., & Bressan, A. 1996, ApJ, 457, 625

Edmunds, M., & Pagel, B., 1984, MNRAS, 211, 507

Elmegreen, B., 1999, ApJ, 517, 103

Flores, H. et al. 1999, ApJ, 517, 148

Fukugita, M., Hogan, C., & Peebles, P.J.E., 1998, ApJ, 503, 518

Gallagher, J., Bushouse, H., & Hunter, D., 1989, AJ, 97, 700

Glazebrook, K., Peacock, J., Miller, L., Collins, C., 1995, MNRAS275, 169

Guzman, R., Gallego, J., Koo, D.C., Phillips, A.C., Lowenthal, J.D., Faber, S.M., Illingworth, G.D., & Vogt, N.P. 1997, ApJ, 489, 559

Guzman, R., 1999, in Proceedings of the XIXth Moriond Conference on "Building Galaxies: from the primordial Universe to the present", ed. F. Hammer, T.X. Thuan, V. Cayatte, B. Guiderdoni & J.T.T. Van (Paris: Editions Frontières),

Hammer, F., Crampton, D., Le Fèvre, O., & Lilly, S.J. 1995, ApJ, 455, 88

Hammer F., et al. 1997, ApJ, 480, 59.

Hammer F., & Flores H, 1998, in Proceedings of the XVIIIth Moriond Conference on "Dwarfs Galaxies and Cosmology", ed. T.X. Thuan, C. Balkowski, V. Cayatte & J.T.T. Van (Paris: Editions Frontières), 353 (astro-ph/9806184)

Hammer, F. 1999, in ASP Conf. Ser., Vol. 197, "Dynamics of Galaxies: from the Early Universe to the Present" eds. F. Combes, G. Mamon and V. Charmandaris (San Francisco: ASP), in press

Jacoby, G., Hunter, D., & Christian, C., 1984, ApJS, 56, 257

Kennicutt, R., Tamblyn, P., Congdon, C., 1994, ApJ, 435, 22

Kennicutt, R. 1998, A&A Rev., 36, 189

Koo, D., & Kron, R. 1981, A&A, 105, 107

Koo, D., Guzman, R., Faber, S., Illingworth, G.D., Bershady, M.A., Kron, R.G., & Takamiya, M. 1995, ApJ, 440, 49

Kobulnicky, H., & Zaritsky, D., 1999, ApJ, 511, 118

Kobulnicky, H., Kennicutt, R., &Pizagno, J. 1999, ApJ, in press

Le Fèvre et al. 2000, MNRAS, 311, 565

Lehnert, M. & Heckman, T., 1996 ApJ, 472, 546

Lilly, S.J., Hammer, F., Le Fèvre, O., & Crampton, D. 1995, ApJ, 455, 75

Lilly S., Le Fèvre O., Hammer F., & Crampton, D. 1996, ApJ, 460, L1

Lilly, S.J., et al. 1998, ApJ, 500, 75

McWilliams, A., 1997, A&A Rev.35, 503

Phillips, A., Guzman, R., Gallego, J., Koo, D., Lowenthal, J.D., Vogt, N.P., faber, S.M., & Illingworth, G.D. 1997, ApJ, 489, 543

Renzini, A., & Cimatti, A., 1999, astro-ph/9910162

Schade, D., et al. 1999, ApJ, 525, 31

Weedman, D. 1983, ApJ, 266, 479

Wheeler, J., Sneden, C., Truran, J., 1989 A&A Rev.27, 279

Williams, R., et al, 1996, AJ, 112, 1335

This 2-column preprint was prepared with the AAS LaTeX macros v5.0.

Table 1: Luminosity and compactness

CFRS	z	M_B	$\frac{L_B}{L_\star}$	Err	M_K	$\frac{L_K}{L_\star}$	Err	L_K[1]	δI^2_{CFHT}	δI^2_{HST}	$\log(r_{1/2})$[3]
03.0442	0.47807	-20.30	0.436	0.064	-21.06	0.254	0.084	2.2	0.68	–	–
03.0523	0.65355	-21.20	1.000	0.147	-22.24	0.752	0.194	6.5	0.43	0.46	0.58
03.0570	0.64682	-20.38	0.470	0.117	—	—	—	—	0.30	–	–
03.0595	0.60442	-20.78	0.680	0.119	-22.09	0.655	0.157	5.6	0.31	0.54	0.65
03.0645	0.52737	-20.77	0.673	0.049	-22.20	0.724	0.113	6.3	0.62	0.64	0.69
03.1242	0.76786	-21.21	1.009	0.223	-22.99	1.500	0.317	12.9	0.73	–	–
03.1349	0.61640	-21.43	1.236	0.114	-23.67	2.805	0.206	24.2	0.73	0.35	0.52
03.1540	0.68931	-21.52	1.343	0.124	-22.83	1.294	0.274	11.2	9999	0.56	0.67
22.0344	0.51680	-20.30	0.437	0.048	—	—	—	—	0.62	–	–
22.0429	0.62433	-20.29	0.433	0.083	-22.13	0.679	0.144	5.9	0.57	–	–
22.0619	0.46706	-20.08	0.356	0.082	—	—	—	—	0.75	–	–
22.0637	0.54188	-21.26	1.057	0.107	-21.83	0.515	0.099	4.4	0.61	–	–
22.0919	0.47144	-20.22	0.406	0.034	—	—	—	—	9999	0.37	0.42
22.1064	0.53685	-20.06	0.350	0.074	-22.43	0.895	0.214	7.7	0.21	–	–

Notes:
[1] in units of 10^{10} $L_\odot$
[2] light concentration, $m_I(15h_{50}^{-1}kpc)$ - $m_I(5h_{50}^{-1}kpc)$; 9999: unsuccessful measurement
[3] $r_{1/2}$ in kpc

Table 2: FWHM of emission lines

CFRS	$FWHM^1_{OII}$	Q^2	$FWHM^1_{H\gamma}$	Q^2	$FWHM^1_{OIII}$	Q^2	$FWHM^1$	Q^2
03.0442	–	9	50	3	50	1	50	1
03.0523	115	2	150	2	180	1	180	1
03.0570	50	3	79.5	3	130	1	130	1
03.0595	54	4	150	2	50	2	50	2
03.0645	50	2	50	2	55	2	55	2
03.1242	135	3	81	3	–	9	108	2
03.1349	252	2	60	2	250	2	250	1
03.1540	50	3	50	3	60	2	60	1
22.0344	–	9	50	2	50	2	50	2
22.0429	52	4	50	3	50	2	50	2
22.0619	50	3	50	2	50	1	50	1
22.0637	89	4	50	2	50	1	50	1
22.0919	–	9	50	1	50	1	50	1
22.1064	–	9	76	2	82	2	80	1

Notes:
[1] In [km/s]
[2] Quality factor: (1) error of 10%, (2) error of 20%, (3) error of 50% and (9) not measured

Table 3: Absorption lines

CFRS	H10	H8	CaIIK	FeI	CN	CaI	FeI	G	FeI	MgI+MgH
λ	3795	3890	3933	4137	4182	4229	4264	4301	4392	5176
03.0442	9999.0	9999.0	9999.0	1.825	4.121	2.232	9999.0	9999.0	5.500	9999.0
03.0523	9999.0	5.262	8.413	0.878	9999.0	1.537	1.972	2.372	8.273	9999.0
03.0570	11.172	9999.0	13.042	3.825	9999.0	6.507	8.937	6.227	10.147	9999.0
03.0595	9999.0	10.948	9999.0	2.843	7.734	2.543	9999.0	9999.0	6.808	9999.0
03.0645	8.185	9999.0	7.354	9999.0	9999.0	1.462	3.613	5.967	5.868	9999.0
03.1242	6.647	9999.0	6.758	6.176	14.247	7.236	10.440	9999.0	13.837	9999.0
03.1349	2.672	9999.0	9999.0	2.031	4.828	3.384	9999.0	3.662	3.640	9999.0
03.1540	9999.0	7.031	5.142	2.660	2.510	3.945	3.836	6.328	7.587	9999.0
22.0344	9999.0	9999.0	9999.0	9999.0	9999.0	3.206	3.202	7.177	9.421	8.239
22.0429	4.091	9999.0	9999.0	2.591	5.497	9999.0	0.314	3.806	9.394	9999.0
22.0619	9999.0	3.185	5.668	0.898	5.983	3.679	4.410	9999.0	6.773	9999.0
22.0637	2.596	4.662	2.309	9999.0	1.107	0.691	0.880	0.833	9999.0	9999.0
22.0919	9999.0	9999.0	9999.0	3.414	1.569	1.751	9999.0	9999.0	3.373	4.118
22.1064	9999.0	9999.0	9999.0	9999.0	3.782	4.684	4.969	3.799	3.081	6.119

Notes:
9999.0: line or continum point used to fit the line is outside the spectral range, or the line is contaminated by the sky

Table 4: LCG stellar populations

CFRS	χ^2	N[1]	age	5×10^9	10^9	5×10^8	5×10^7	10^7	10^6
03.0442	0.029	4	$Z/Z_\odot$[2]	-1.0	-0.5	—	-0.5	-0.5	—
			%	15	**75**	0	5	5	0
03.0523	0.250	5	$Z/Z_\odot$	—	0.6	—	—	-0.5	—
			%	0	**50**	0	0	**50**	0
03.0570	0.361	5	$Z/Z_\odot$	0.6	0.6	—	-0.5	—	—
			%	10	**80**	0	10	0	0
03.0595	0.229	5	$Z/Z_\odot$	-1.5	0.6	—	—	-0.5	—
			%	25	**60**	0	0	15	0
03.0645	0.471	6	$Z/Z_\odot$	-1.5	0.6	—	—	-0.5	0.0
			%	35	**50**	0	0	10	5
03.1242	1.530	6	$Z/Z_\odot$	—	0.6	—	—	-0.5	—
			%	0	**95**	0	0	5	0
03.1349	0.286	5	$Z/Z_\odot$	-1.5	0.6	—	—	—	0.0
			%	**50**	30	0	0	0	20
03.1540	0.915	6	$Z/Z_\odot$	-1.5	-0.5	—	—	—	—
			%	10	**90**	0	0	0	0

Notes:
[1] Number of absorption lines used for the fit
[2] in logarithmic unit

Table 4 (continued): LCG stellar populations

CFRS	χ^2	N[1]	age	5×10^9	10^9	5×10^8	5×10^7	10^7	10^6
22.0344	1.836	5	$Z/Z_\odot$	-1.5	0.6	—	—	-0.5	—
			%	15	**70**	0	0	15	0
22.0429	0.100	4	$Z/Z_\odot$	—	0.6	—	—	-0.5	0.0
			%	0	**55**	0	0	40	5
22.0619	0.420	5	$Z/Z_\odot$	0.6	-1.0	—	—	—	0.0
			%	**55**	10	0	0	0	35
22.0637	0.296	7	$Z/Z_\odot$	-1.5	-1.0	—	—	-0.5	0.0
			%	35	20	0	0	**55**	10
22.0919	0.167	4	$Z/Z_\odot$	—	-1.0	—	-0.5	-0.5	—
			%	0	**90**	0	5	5	0
22.1064	0.466	5	$Z/Z_\odot$	—	-0.5	—	—	-0.5	—
			%	0	**95**	0	0	5	0

Notes:
[1] Number of absorption lines used for the fit
[2] in logarithmic unit

Table 5: Extinction and SFR

CFRS	$\frac{H\beta}{H\gamma}$	Err	A_v	Err	SFR^1_{2800}	$SFR^2_{H\alpha}$	Err
03.0442	2.64	0.52	1.53	$^{+1.30}_{-1.53}$	1.52	11.54	$^{+11.91}_{-2.70}$
03.0523	2.68	0.24	1.65	$^{+0.62}_{-0.68}$	4.20	107.35[3]	$^{+63.05}_{-31.90}$
03.0570	2.18	0.43	0.15	$^{+1.30}_{-0.15}$	1.80	3.27	$^{+6.52}_{-1.48}$
03.0595	2.45	0.48	1.00	$^{+1.30}_{-1.00}$	2.00	18.70	$^{+32.23}_{-7.30}$
03.0645	2.64	0.17	1.54	$^{+0.46}_{-0.49}$	3.33	37.76	$^{+9.34}_{-5.67}$
03.1242	–	–	–	–	—	–	–
03.1349	2.98	0.45	2.42	$^{+1.01}_{-1.18}$	3.79	134.38[3]	$^{+151.16}_{-48.25}$
03.1540	3.04	0.36	2.56	$^{+0.82}_{-0.93}$	4.39	88.50[3]	$^{+90.79}_{-36.20}$
22.0344	2.76	0.22	1.86	$^{+0.56}_{-0.61}$	1.67	27.57	$^{+8.61}_{-4.64}$
22.0429	–	–	–	–	–	–	–
22.0619	2.29	0.22	0.51	$^{+0.66}_{-0.51}$	1.04	9.62	$^{+3.00}_{-1.46}$
22.0637	2.37	0.19	0.76	$^{+0.56}_{-0.61}$	3.69	5.25	$^{+1.84}_{-0.99}$
22.0919	2.25	0.08	0.38	$^{+0.27}_{-0.28}$	2.41	8.42	$^{+0.86}_{-0.64}$
22.1064	2.78	0.19	1.91	$^{+0.48}_{-0.51}$	1.61	37.66	$^{+10.25}_{-6.09}$

Notes:
[1] SFR in [M$\odot/yr$], without correction for extinction
[2] SFR in [M$\odot/yr$] corrected from extinction calculated from the $H\beta/H\gamma$ ratio
[3] also detected by ISO (Flores et al, 2000, in preparation).

Table 6: Gas properties

CFRS	$log(R_{23})^1$	R^2_{ion}	OIII ratio[3]	T_{gaz}[K]	e(T)[4]	$\frac{O}{H}{}^5_1$	$\frac{O}{H}{}^5_2$	$\frac{O}{H}$	Err
03.0442	1.10	0.22	65	15000	3	8.2	8.4	8.3	0.1
03.0523	0.76	0.57	233	11000	3	8.0	8.5	8.3	0.2
03.0570	0.69	0.76	149	12000	3	7.9	8.7	8.3	0.5
03.0595	0.31	0.30	50	18000	3	7.6	8.9	8.3	0.6
03.0645	0.79	0.56	111	12500	3	8.3	8.55	8.4	0.15
03.1349	0.60	0.59	174	11500	3	8.0	8.8	8.4	0.4
03.1540	0.57	0.05	30	22000	3	8.2	8.9	8.5	0.3
22.0344	0.67	0.31	119	12500	3	8.0	8.8	8.4	0.4
22.0619	0.87	1.54	116	12500	2	8.3	8.2	8.2	0.05
22.0637	0.72	0.58	75	14500	3	8.2	8.6	8.4	0.2
22.0919	0.86	33.24	105	13000	1	7.8	8.8	7.8	0.05
22.1064	0.73	0.97	40	21000	3	7.85	8.8	8.3	0.5

Notes:
[1] See text.
[2] Ionization
[3] $[OIII]5007 + [OIII]4959/[OIII]4363$ ratio
[4] Quality factor: 1 excellent, 2 estimated, 3 temperature limit
[5] O/H : 1 lower value and 2 higher value (cf. Kobulnicky, 1999)

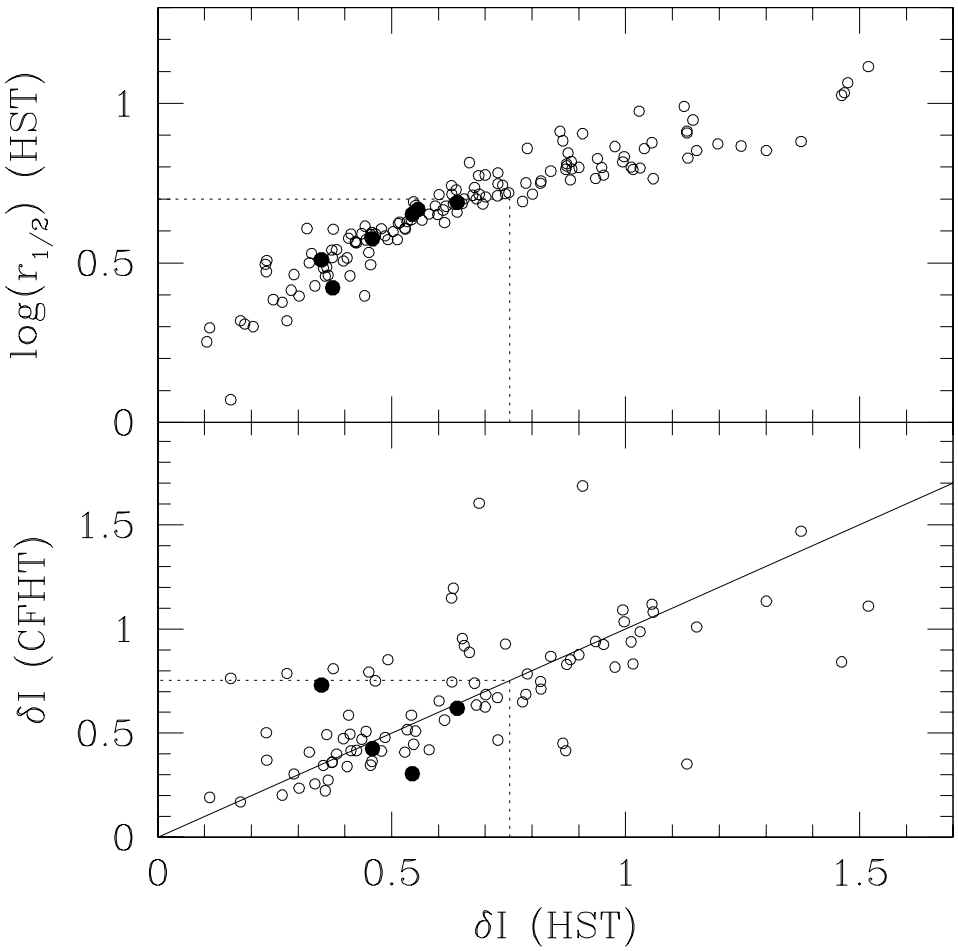

Fig. 1.— Compactness selection criteria for Luminous Compact Galaxies (LCG). *Top*: logarithm of half-light radius $r_{1/2}$ (in kpc) against light concentration parameter for galaxies observed with HST/WFPC2 in the F814W filter; filled dots show the 6 LCGs (CFRS 03.523, CFRS 03.0595, CFRS 03.0645, CFRS 03.1349, CFRS 03.1540 and CFRS 22.0919) in this paper imaged with the HST. The dotted lines delimit the compact galaxy area. CFRS 03.523 is made of two very close components and was classified as a merger by Le Fèvre et al (2000). *Bottom*: comparison between the light concentration parameter derived from ground-based images (FWHM = 0".7) and that derived from HST images. CFRS 03.1540 and CFRS 22.0919 have ground-based images which aperture magnitudes showing a decrease in brightness with the aperture radius decreasing from 3" to 0.2". Their concentration parameter cannot be derived, probably because of the presence of a companion which was not properly masked. In the absence of HST imagery, those two galaxies would have been excluded from our sample.

Fig. 2.— **JPEG enclosed** *Left*: Ground-based Canada-France-Hawaii telescope images of the 14 LCGs in the sample, with the slit superimposed. *Right*: The 6 LCGs in the sample observed by WFPC2/HST. HST image quality reveals low surface brightness extents and closeby interactions , generally not detectable from the ground.

Fig. 3.— **JPEG enclosed** Rest-frame VLT spectra of the 14 LCGs in our sample. The continuum has been smoothed first by 7 pixels and then by 15 pixels, giving a spectral resolution of 11 Å, except at the location of the emission lines ([OII]3727, $H\epsilon$, $H\delta$, $H\gamma$, $H\beta$, [OIII]4959 and 5007) for which the rest-frame spectral resolution is 3.5 Å. Pairs of vertical dashed lines delimit the regions where strong sky emission lines (OI 5577, 6300 and 6364 Å) or absorption lines (O2 6877, 7606 and 7640 Å) severely affect the continuum. The main absorption lines are indicated and their identifications are given in the last panel. The latter shows an enlargement of the CFRS 03.1540 spectrum, as well as the adopted fit for its continuum (solid line), used to calculate the absorption line equivalent widths (see section 4.2).

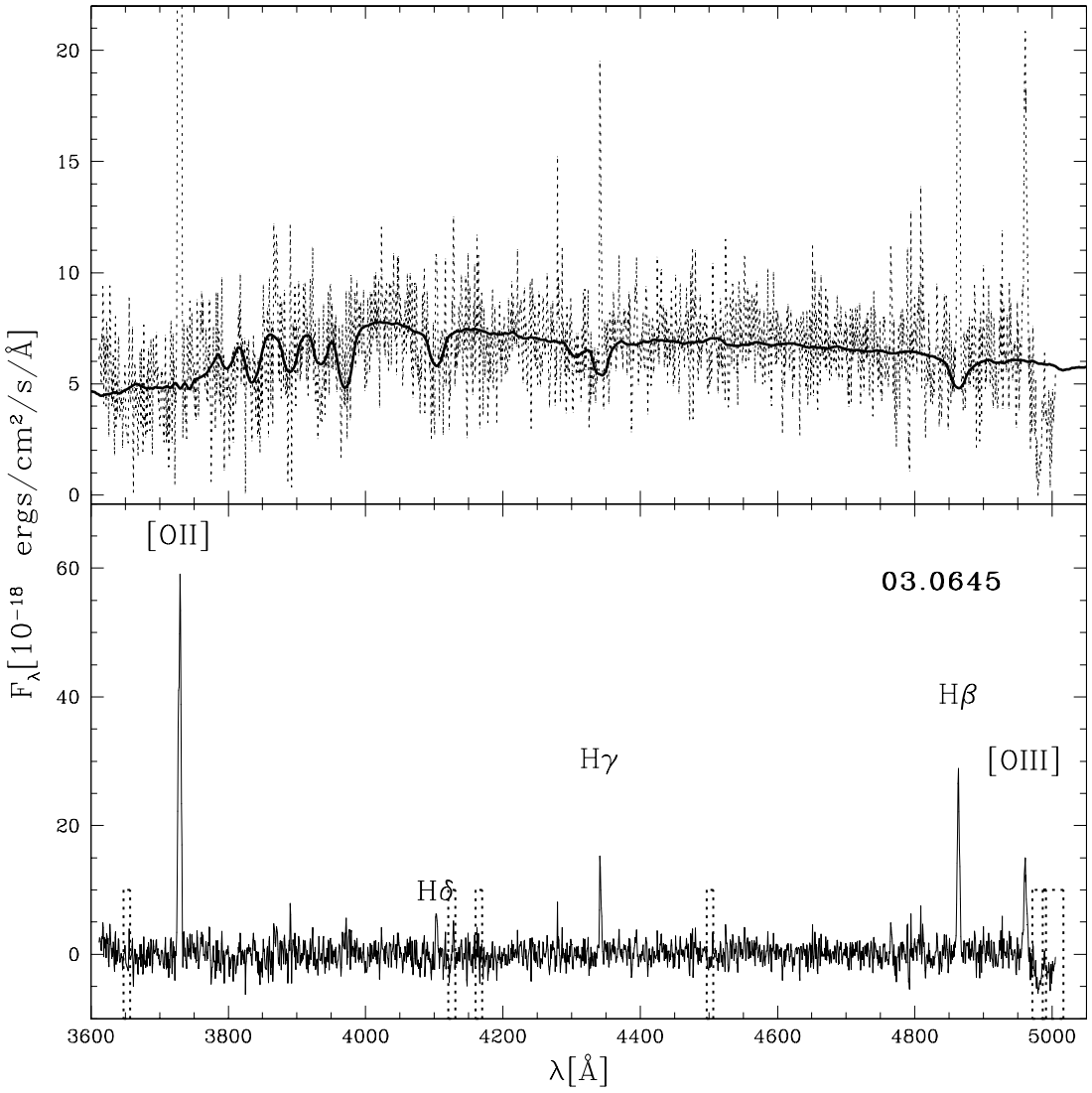

Fig. 4.— *Top*: Rest-frame spectrum of CFRS 03.0645 without smoothing on which a synthesized spectrum resulting from the combination of B V (contributing 22% of the light), A V (20%), F V (42%) and G V stars (16%) is superimposed (bold line). *Bottom*: emission line spectra of CFRS 03.645 after removal of the stellar continuum as determined from spectral synthesis. Pairs of vertical dashed lines delimit the regions where strong sky emission or absorption affect the continuum.

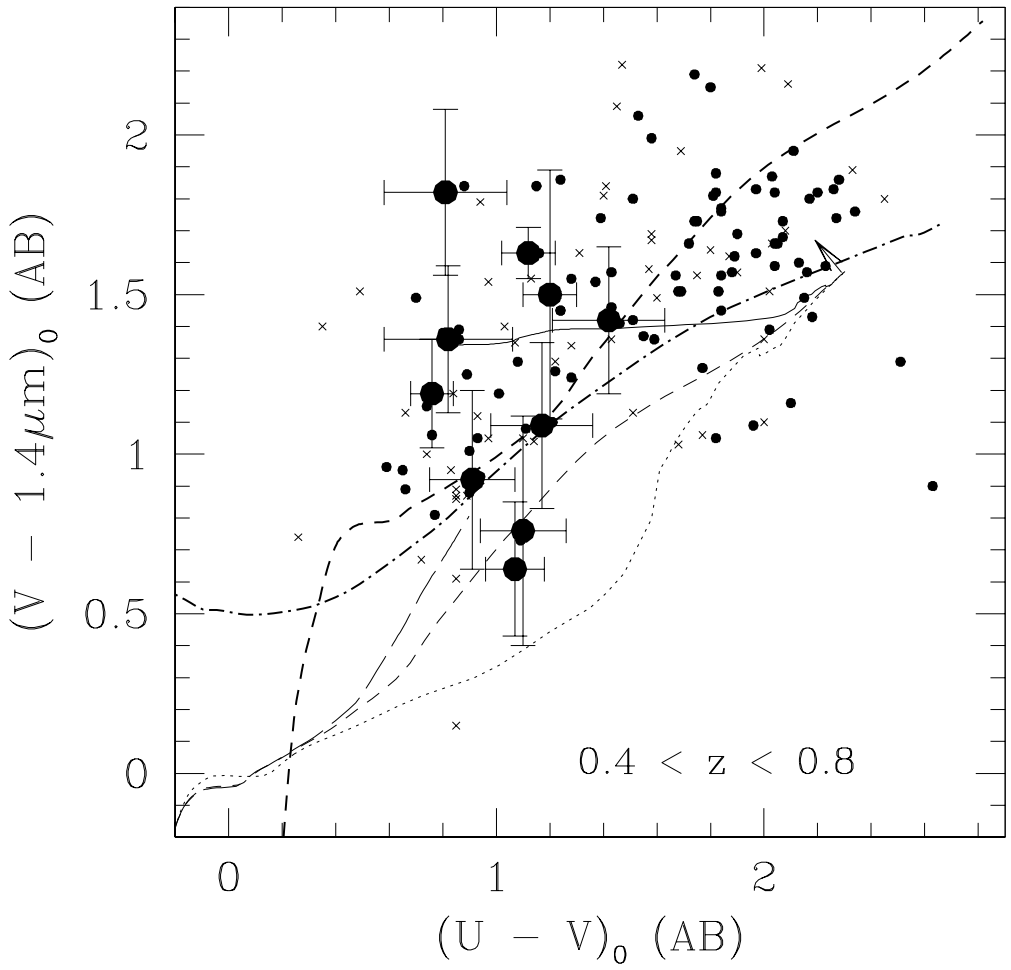

Fig. 5.— Rest-frame color $(V - 1.416\mu\mathrm{m})_{AB}$ versus $(U - V)_{AB}$ for CFRS luminous galaxies ($M_B \leq$ -20). Small dots represent LCGs with or without emission lines, including ellipticals. Small crosses represent galaxies which are not compact. Large dots show the 10 galaxies in our sample of 14 LCGs which have near-IR photometric measurements. Error bars are mainly due to observational errors (see text). Lines show Bruzual and Charlot (1999) models with solar metallicity and an exponential declining SFR with an e-folding time-scale τ. The dotted line show the model with $\tau = 0.1$ Gyr, the short-dashed line the model with $\tau =$ 1 Gyr and the long-dashed line the model with a constant SFR. The bold short-dashed line represents the τ=1 model with an extinction $A_V = 1$ applied. The bold dot-short dashed line represents the $\tau = 1$ Gyr model, assuming a metallicity $Z/Z_\odot = 3.2$. A composite model, where 80% of the light is contributed by an old stellar population formed 10 Gyr ago in an instantaneous burst, and the remaining 20% of the light by a younger stellar population with $\tau = 1$ Gyr, is shown as a solid line. It can be seen that, because of their large $(V - 1.4\mu\mathrm{m})_{AB}$, several LCGs in our sample require either extinction, population mixing, over-solar abundances or a combination of the above. A small arrow on the upper-right side of the Bruzual and Charlot (1999) models indicates the uncertainties in the modeling of the old stellar population, as discussed by Charlot et al. (1996).

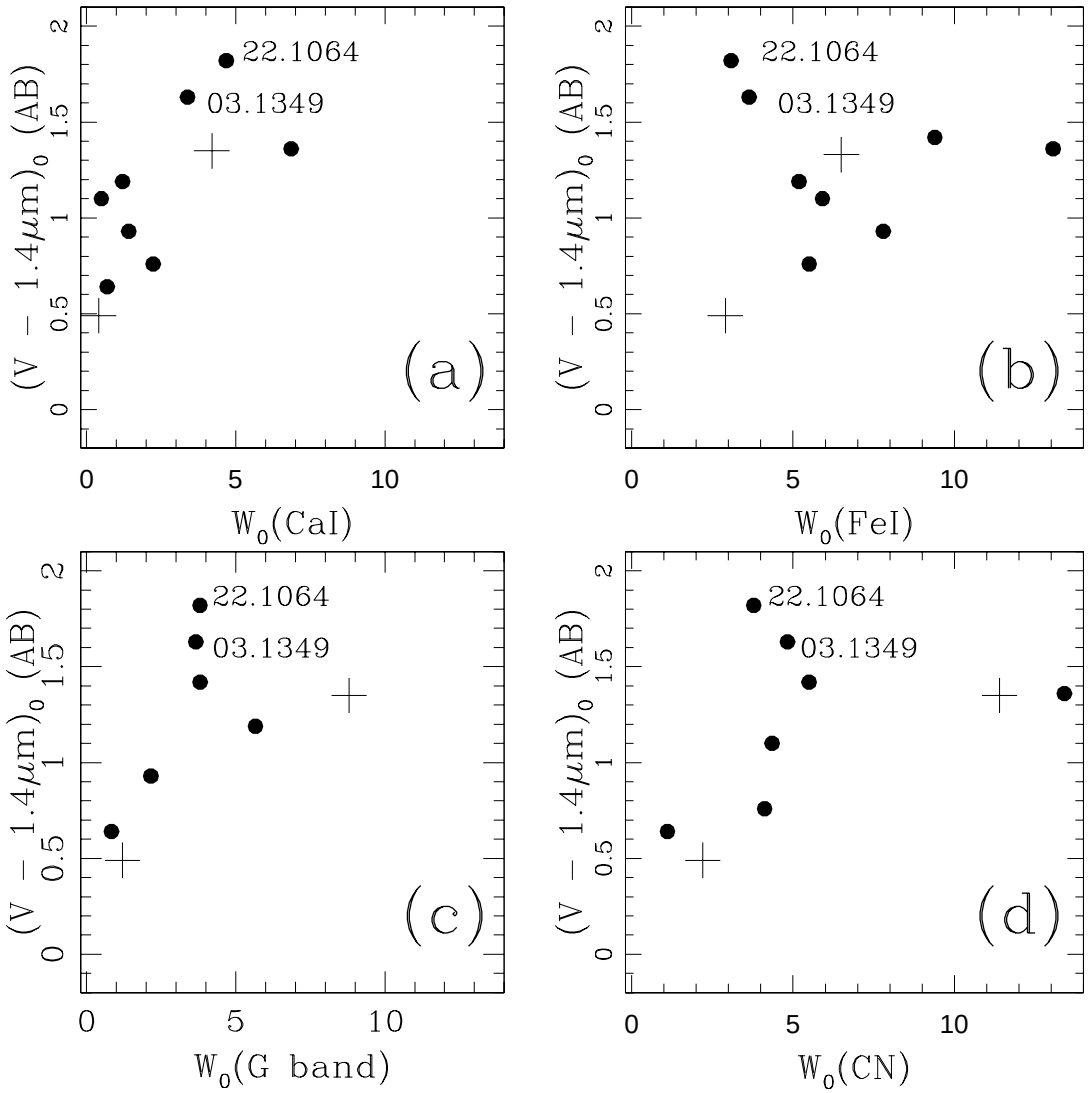

Fig. 6.— $(V-1.4\mu\mathrm{m})_{AB}$ color index against equivalent widths of a) CaI 4227Å, b) FeI 4384Å, c) CH (G band at 4301Å) and d) CN band at 4182Å. Red $(V-1.4\mu\mathrm{m})_{AB}$ colors are related to strong metallic absorption lines, i.e. either to large abundances or to old stellar populations. At least two galaxies, CFRS 03.1349 and CFRS 22.1064, deviate from the relationship, probably because their color indices are significantly affected by extinction. In each panel the two crosses represent the properties of stellar clusters with solar metallicity, with ages of 5 Gyr (upper right) and 0.1 Gyr (bottom left) respectively. Comparison of the locations of the filled dots relative to the crosses in the four panels illustrates the fact that most LCG properties can be fitted by a mix of a solar abundant old stellar population with a young population.

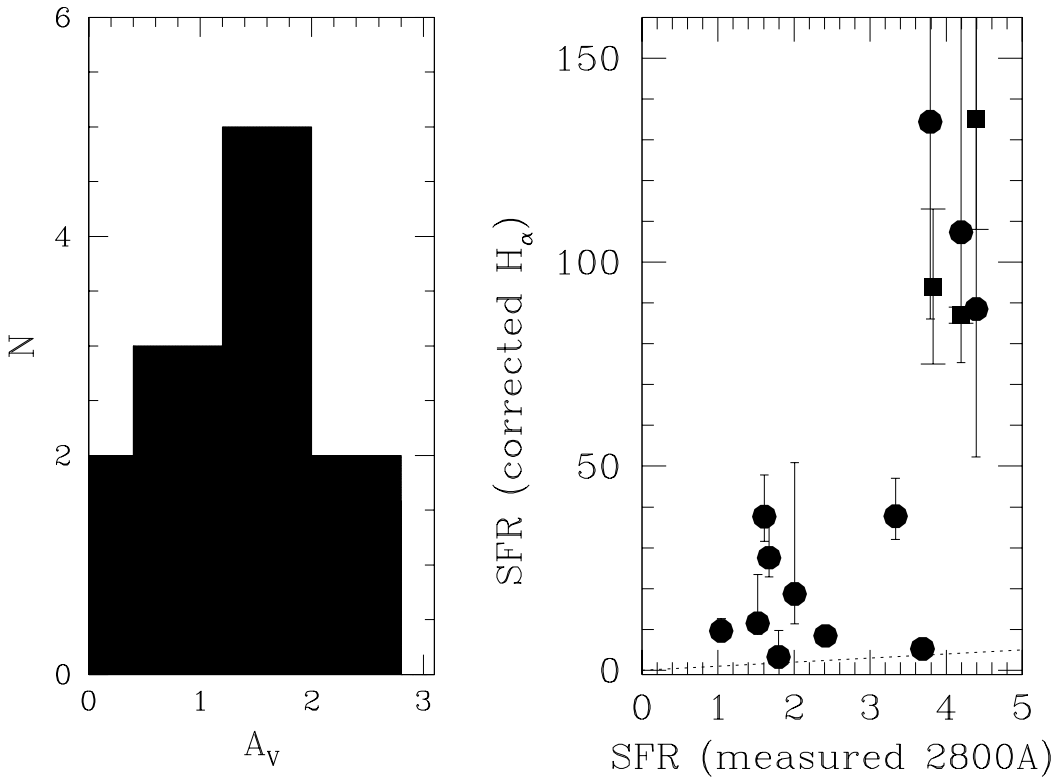

Fig. 7.— *Left*: Histogram of the extinction coefficient A_V as derived from the $H\beta/H\gamma$ ratio. The signal-to-noise ratio of the $H\gamma$ line ranges from 10 to 30, which leads to a 1 σ error of 0.5 to 1 mag on A_V (see Table 5). *Right*: The SFRs derived from dereddened Balmer emission lines compared to those derived from 2800Å luminosities not corrected for extinction. Vertical error bars represent 1σ uncertainties, mostly due to the extinction corrections. For three LCGs, CFRS 03.0523, CFRS 03.1349 and CFRS 03.1540, the global SFR has been also calculated from the fit of their spectral energy distribution from UV to radio wavelengths, including ISO mid-IR measurements (see text). These three estimates are represented by squares, which are consistent with estimates from extinction corrected Balmer lines (full dots located at the same SFR_{2800} value).

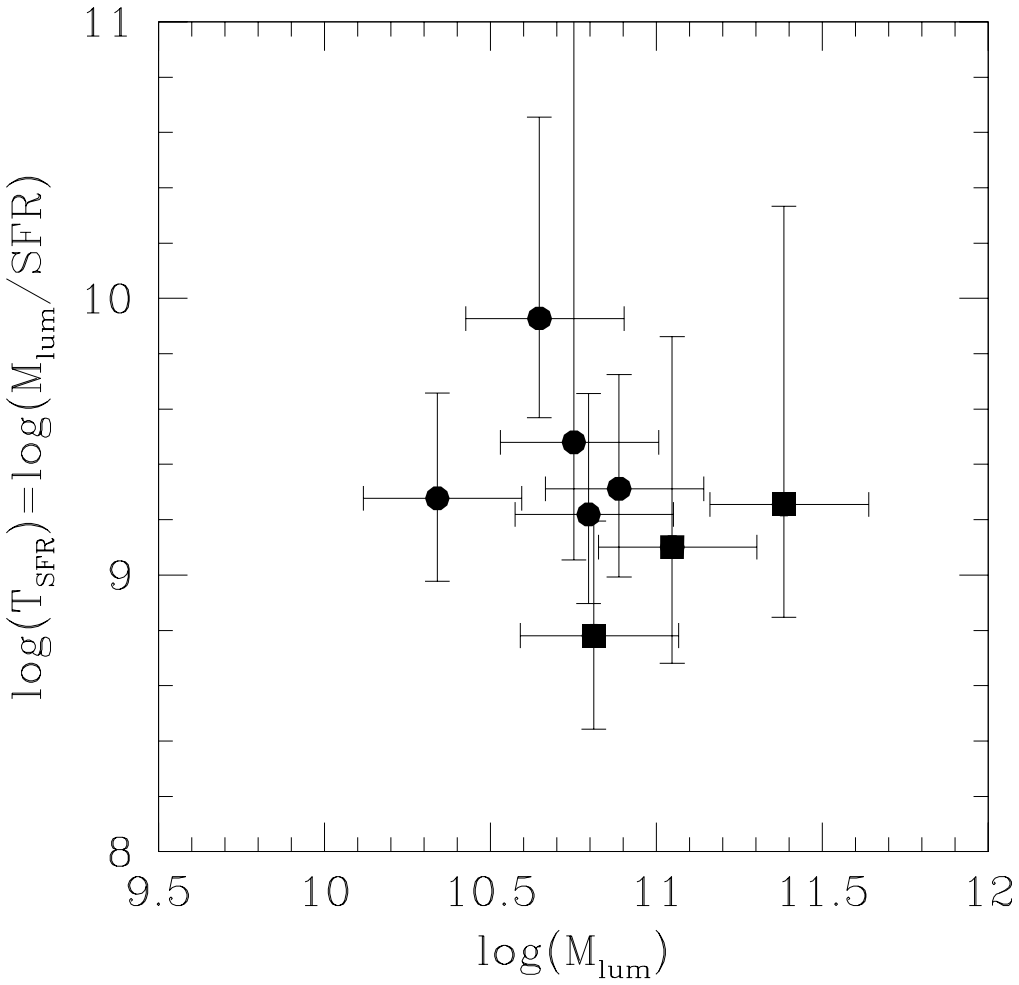

Fig. 8.— Logarithm of the ratio between the luminous mass and the global SFR against the logarithm of the luminous mass. The former ratio is the required time T_{SFR} to form the bulk of the LCG stars, assuming that star formation is sustained at the observed value. Luminous masses have been derived from the K-band luminosity while the SFRs have been derived either from the dereddened Balmer emission line fluxes or by fitting the global spectral energy distribution (squares). A mass-to-light ratio $M_K/L_K = 1$ has been assumed to derive the luminous mass. Vertical error bars represent the full range of values that this ratio can take, from 0.6 to 1.8, assuming a burst older than 0.1 Gyr (Charlot 1999). Horizontal error bars show the 1σ error on the SFR estimate.

This figure "Figure2.jpg" is available in "jpg" format from:

http://arxiv.org/ps/astro-ph/0011218v1

This figure "Figure3a.jpg" is available in "jpg" format from:

http://arxiv.org/ps/astro-ph/0011218v1

This figure "Figure3b.jpg" is available in "jpg" format from:

http://arxiv.org/ps/astro-ph/0011218v1